IMPACT OF AMBIENT NOISE AND SHIP TONALS ON THE INVERSION OF SEAFLOOR REFLECTIVITY FROM RANGE-FREQUENCY STRIATIONS IN SHALLOW OCEANS

AD Jones Defence Science and Technology Organisation Edinburgh, SA 5111, Australia
DW Bartel Defence Science and Technology Organisation Edinburgh, SA 5111, Australia
PA Clarke Defence Science and Technology Organisation Edinburgh, SA 5111, Australia

1 INTRODUCTION

It is well known that sound transmission to short and medium ranges in shallow oceans is highly dependent upon the seafloor reflective properties. The multiple paths/multiple modes of acoustic transmission combine constructively and destructively such that sound transmitted over a broad frequency band forms a pattern of lines, known as "striations", when amplitude levels at each range are plotted against frequency on a range-frequency plot. As previously presented by the authors[1], the frequency spacing of the striations may be used to invert the seafloor reflective properties for small angles of grazing incidence, and[2] by averaging along the striations, the broadband data received from a ship-of-opportunity may be used. For practical use, the technique is limited by the contamination of the striation data by the prevailing level of ambient ocean noise, and may be limited by levels of tonals received from either the ship-of-opportunity, or by another source. The issues and details of such limitations are the subject of this paper.

An example of a range-frequency plot showing striations is shown in Figure 1 for a simulation with a seafloor half-space of coarse sand. Here, Transmission Loss (*TL*) is shown in 10 m steps of horizontal range to 4000 m, and in 1 Hz steps of frequency to 500 Hz. The wavenumber-integral model HANKEL[3] was used for these simulations. The ocean was simulated as isovelocity (1500 m/s), of depth 80 m with both source and receiver at 18 m, seafloor compressional speed and attenuation 1800 m/s and 0.7 dB/λ, shear speed and attenuation 600 m/s and 1.5 dB/λ, and density was twice that of seawater (geoacoustic parameters from Jensen and Kuperman's[4] Table 1).

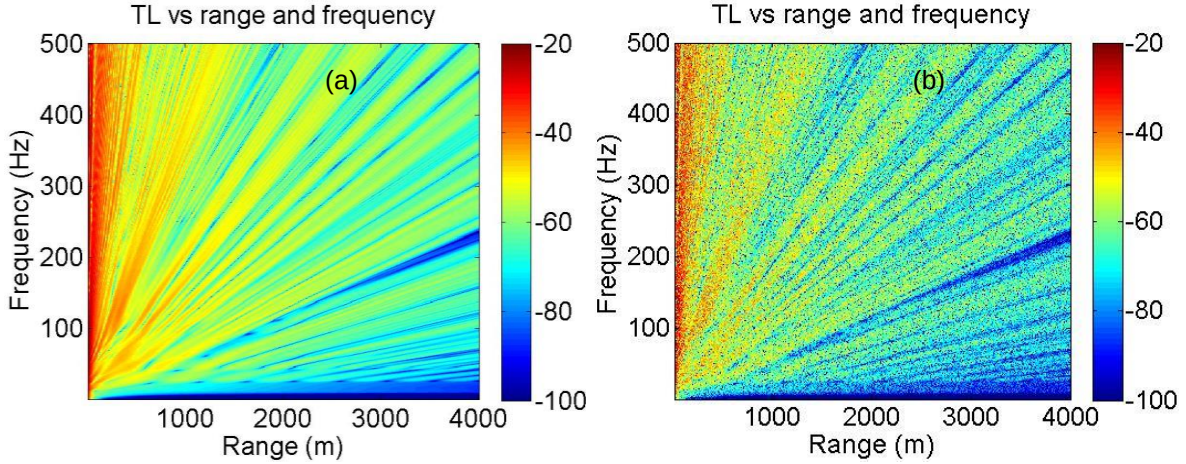

Figure 1 Simulated range-frequency Transmission Loss, for 80 m ocean, coarse sand seafloor, range data at 10 m intervals (a) coherent source, (b) random source

Figure 1 (a) simulates the *TL* for a coherent source at successive distances from the receiver, and is identical to the received signal from a source of Source Level (*SL*) 0.0 dB dB re $(1\mu\text{Pa})^2$. In practice, these data are a series of spectra received at subsequent times from a moving source. As the source-receiver relative movement over the time for the summation of the multi-paths (duration

of order τ, mentioned later) is very small, the relative amplitude distribution across each received spectrum is unaffected by the speed of the source. For a broadband source of opportunity, e.g. a passing ship, the source signal has no temporal coherence, and resembles random noise. Figure 1 (b) simulates the data received from such a random source, for the same scenario. Here each spectrum at each range value contains a value in each frequency bin which is an uncorrelated Gaussian value about a mean determined by the multi-path combination. Each of these random samples may be averaged according to the bandwidth-time product implied by temporal and spectral sampling. For the particular example in the figure, the frequency data is at an interval of 1 Hz, and so the broadband *SL* of the data in part (b) is 0.0 dB re $(1\,\mu\text{Pa})^2/\text{Hz}$.

2 INVERSION ALONG STRIATIONS

2.1 Range-Frequency Striations In A Shallow Ocean

The occurrence of range-frequency striations in data received in a shallow ocean may be understood by examining the phase coherent addition of multi-path arrivals. A phase change between the ray arrivals due to a change in frequency is equivalent to a phase change between the same arrivals due to a change in source to receiver range, with a constant of proportionality which, to a very good approximation, varies linearly in frequency and inversely in range. The phase relationship between two arrivals may then be held at zero if the frequency is increased by δf and the range increased by $(r\,\delta f)/f$. A consequence is that $\delta f/\delta r \approx f/r$ along the region of unchanged phase separation, and "striations" appear on the range-frequency plot. If the axes are linear, the striations appear on the plot as straight lines originating from *f* = 0, *r* = 0, as in Figure 1. The above assumes that (i) there are enough modes to describe a continuous variation of grazing angles for the multi-path arrivals, and (ii) the rate of change of the phase difference with range $d\phi/dr$ is dominated by transmission path length effects. The relation $\delta f/\delta r = f/r$ is commonly expressed in terms of angular frequency $\omega = 2\pi f$ as

$$(r/\omega)[d\omega/dr] = \beta \qquad (1)$$

where β is an invariant for a waveguide[5], but is not necessarily of value exactly 1.0 as implied here.

2.2 Frequency Variability-Based Inversion

A technique for inversion of seafloor reflectivity is described by Jones et al.[1]. This may be considered as a frequency-domain variant of the channel impulse response technique described by Smith[6] and used by Prior and Harrison[7]. Both techniques exploit the approximation of the channel impulse response function as exponential for which the time constant may be expressed in terms of the shallow ocean depth *D* and the value *F* dB/radian, the presumed function of bottom loss vs. grazing angle for small grazing angles. For an isovelocity ocean, the impulse decay time constant may be shown to be $\tau \approx [10\log_{10}(e)]D/(c_w F)$ seconds, where c_w is the speed of sound in seawater. The concept of a near-constant value of bottom loss versus grazing angle, *F* dB/radian, for small grazing angles, is well known[8]. The parameter *F* is identical to the term α_{dB} of Prior and Harrison[7].

As shown by Schroeder[9], for a transmission environment with an exponential decay of the intensity impulse, the spectral autocorrelation function of the received sound pressure amplitude is

$$\rho_{|p|}(\Delta f) = 1/\left[1+(2\pi\tau\,\Delta f)^2\right] \qquad (2)$$

where Δf , is the frequency displacement (Hz) for a specified de-correlation. For convenience with practical data, it was decided to use the value Δf_h being the frequency displacement at which the autocorrelation falls to 0.5. From (2), $\Delta f_h = 1/(2\pi\tau)$ Hz. Substituting for τ gives

$$\Delta f_h \approx \ln(10)c_w F/(20\pi D) = 0.037 F c_w/D \text{ Hz}. \qquad (3)$$

The bottom loss parameter *F* follows as

$$F \approx 27.3 D \Delta f_h / c_w \text{ dB/radian.} \qquad (4)$$

With a measured striation pattern, the frequency spacing of features is processed to determine values of Δf_h. (Approximately, average spacing between frequency maxima is about $3\Delta f_h$ Hz[2].) The processing used by the authors determines the spectral autocorrelation of the received sound pressure amplitude values expressed about a zero mean, with the value Δf_h corresponding with an autocorrelation of 0.5. Based on an inverted value of *F* dB/radian, an accompanying approximation for reflection phase may be made (e.g. Jones et al.[10]), and so reasonable estimates of phase coherent sound transmission may be obtained through use of a suitable transmission model.

2.3 Averaging Frequency Data Along Striations

The determination of Δf_h from data received from a single random source in a noise background benefits from averaging the mean-squared spectral pressure data received at different range points prior to the frequency autocorrelation. A method was devised to perform this averaging along the slope of the striations[2], which for a channel invariant of 1.0 are assumed to follow straight lines radiating from $f = 0$, $r = 0$. Figure 2 shows the bounds used for such "matched-slope" averaging, in which the mean-squared pressure values at each frequency between f_1 and f_2, starting at range r_1, are averaged along each respective striation, this being a corresponding straight line from $f = 0$, $r = 0$, to range r_2. For the purposes of carrying out the autocorrelation on the spectrum resulting from this averaging, the averaged value corresponding with each striation is assigned the frequency value corresponding to range r_1. Now, the frequency spacing of features in the spectrum between f_1 and f_2 scales with Δf_h, and is unchanged with range as implied by Equation (4). However, the band of frequencies subject to the averaging, enclosed between the lines A and B in Figure 2, increases with range, and so the spectrum features within this band will change if the distance r_1 to r_2 is not small. In particular, it may be anticipated that a tolerable increase Δf_2 in the band of frequencies (see Figure 2) is achieved if the averaging is limited to a span of range values Δr so that $\Delta f_2 \le \Delta f_h$. This is reasonable as, on average, the amplitudes of spectral values in the channel response have a correlation of 0.5 at the frequency separation Δf_h.

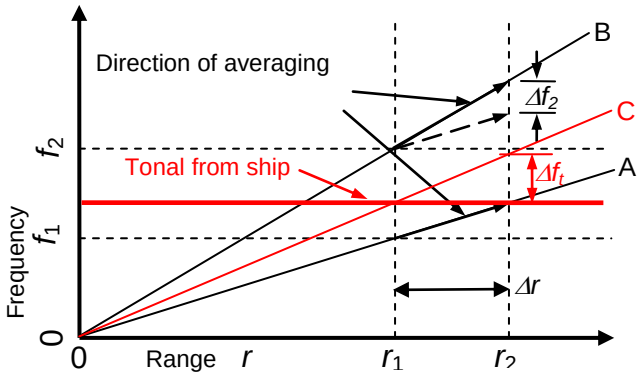

Figure 2 Striations on range-frequency plot and implications for matched-slope averaging

Now

$$\Delta f_2 = (r_2 - r_1)(f_2 - f_1)/r_1 . \qquad (5)$$

If the slopes of the striations A and B are assumed to be not greatly different, and if the range and frequency extents $r_2 - r_1$ and $f_2 - f_1$ are not large relative to absolute values, it is possible to make some substitutions using $\delta f / \delta r = f / r$. In particular, $(r_2 - r_1)/(f_2 - f_1) \approx r_2/f_2 \approx r_1/f_1 \approx r/f$, and

$f(r_2 - r_1)/r$ may be substituted for $f_2 - f_1$ in (5) to give $\Delta f_2 \approx f(r_2 - r_1)^2 / r^2$. Making the substitution $\Delta f_2 < \Delta f_h$, and obtaining Δf_h from (4), the range limit for averaging Δr may be found as

$$r_2 - r_1 = \Delta r < r\sqrt{\Delta f_h / f} = \Delta r < r\sqrt{0.037 c_w F/(Df)}. \qquad (6)$$

In practice, it is preferable to remove the mean variation of *TL* with range from the data before the matched-slope averaging is carried out. From section 3, this mean trend approximates $15\log r$.

2.4 Range-Based Inversion Using Data at Single Frequency

As the variations in signal amplitude with range and frequency are related by $\delta f/\delta r \approx f/r$, and the frequency scale of amplitude variability is Δf_h, for each particular frequency there is a corresponding range scale of amplitude variability $\Delta r_h = r\,\Delta f_h / f$. From Equation (3) it follows that

$$\Delta r_h = 0.037 F c_w\, r/(f D). \qquad (7)$$

This may be inverted to determine the reflectivity parameter *F*, as

$$F \approx 27.3 Df\, \Delta r_h/(r\, c_w) \text{ dB/radian} \qquad (8)$$

and the inversion for *F* may be accomplished by processing the tonal data received over a span of ranges from the source ship-of-opportunity. As the value of Δr_h in Equation (8) is linearly related to range *r*, the range spacing of the data must be normalized to that relevant at a nominal range value associated with the averaging, before the autocorrelation of the received sound pressure amplitude values is carried out to obtain Δr_h. Of course, it is also desirable to remove the mean variation of *TL* with range from the data. Such inversion has been conducted, but is not described in this paper.

3 SIGNAL FROM SHIP-OF-OPPORTUNITY

For transmission to ranges of the order 2 km to 4 kms in an ocean of depth 80 m, it is reasonable to assume an isovelocity sound speed profile, as the angles of incidence of multi-paths at the sea surface and seafloor are much greater than angular deviations of multi-paths due to refraction. The *TL* at range *r* m, energy-averaged over the ocean depth, may be obtained by adding the contribution from multi-path arrivals using the method of images. Urick[11], for example, obtained

$$TL = 15\log r + 5\log(F D) - 6.79 \text{ dB}. \qquad (9)$$

Due to multi-path interference, the phase-coherent signal amplitude will undergo fluctuations about the energy-averaged *TL* given by Equation (9), and these fluctuations will be, approximately, Rayleigh-distributed. Fluctuations occur with changes in any of range, depth and frequency.

A ship-of-opportunity may be assumed to have a broadband *SL* at 1 m according to a mean-squared pressure spectral density of B $(\text{Pa})^2/\text{Hz}$ for frequencies near *f* Hz. Likewise, it may be assumed that a tonal at frequency *f* has a mean-squared pressure of T $(\text{Pa})^2$ referenced to 1 m. At range *r* m, the received broadband signal amplitude will be Rayleigh distributed with a frequency scale given by Δf_h, and the energy-averaged received levels of broadband and tonal signal are in accord with mean-squared pressures $B_r = B/10^{(TL/10)}$ $(\text{Pa})^2/\text{Hz}$ and $T_r = T/10^{(TL/10)}$ $(\text{Pa})^2$.

3.1 Interference from Ship Tonal

Matched-slope processing of data including a tonal is illustrated by the material in Figure 2 in red. In averaging between the lines A and C, the intensity in the tonal is spread over a frequency band Δf_t Hz at range r_2, which from Equation (1) is $f\,\Delta r/r$ Hz. Depending on the slope of the lines A

and C, at range r_2 the energy from the tonal will at most be spread over the full band of frequencies $f_2 - f_1 + \Delta f_2$ Hz, but more commonly Δf_t will be a sub-set of this span. Over the band Δf_t, the tonal may interfere with the receipt of the broadband signal from the ship-of-opportunity. In relation to the matched-slope averaging, the tonal at range r_2 causes interference according to a mean-squared pressure $T_r / \Delta f_t \approx T r / \left(f \, \Delta r \, 10^{(TL/10)} \right)$ $(\text{Pa})^2/\text{Hz}$. Relative to the decrease in the level of a broadband signal at the same range, this represents a decrease in interference by the factor $f \, \Delta r / r$, that is by $10 \log_{10} \left(f \, \Delta r / r \right)$ dB. Using the description in Equation (6) of the maximum value for Δr, the maximum reduction in interference may be stated as $5 \log_{10} \left(f \, \Delta f_h \right)$ dB.

If the source of the tonal is co-located on the ship-of-opportunity with the source of the broadband signal, the transmission multi-paths will be identical for both the tonal and broadband data, and the range-frequency fluctuations will be fully correlated for both signal types. Sources much further apart than the range scale of amplitude variability, Δr_h, will have uncorrelated range and frequency fluctuations, and the associated received tonal and broadband signals will interefere during matched-slope averaging. For measurements at a nominal range of 3750 m, for an ocean depth of 80 m, from Equation (7), $\Delta r_h \approx 2600 F / f$ metres. For 200 Hz, for example, values of Δr_h vary between 65 m for $F = 5$ dB/radian (reflective seabed) to 650 m for $F = 50$ dB/radian (absorptive seabed). The sources may be presumed co-located if separated by radial distances of << Δr_h, but the signals received from them will interfere if the separation is by more than Δr_h.

4 DEMONSTRATION OF FREQUENCY VARIABILITY-BASED INVERSION TECHNIQUE - SIMULATION

In prior work[2], matched-slope averaging was applied to the range-frequency data shown in Figure 1 (b), from 75 Hz to 500 Hz and over rages from 3500 m to 4000 m. The use of data over a large frequency span was permissible as the reflectivity of a uniform half-space may be anticipated to be frequency independent. From the matched-slope averaged data, repeated in Figure 4 (b) below, the value of Δf_h was obtained by an autocorrelation of the amplitude data. Then from (4), the bottom loss vs. grazing angle slope F was determined, and found to be very close to the known value of 10 dB/radian, where the latter had been obtained from a layered-media reflection model, using data from 0° to 10° grazing angle. With range steps of 10 m, 50 sets of spectral data were averaged prior to the autocorrelation used to determine Δf_h. The lower frequency limit of 75 Hz was based on an estimate that multi-modal transmission (about 5 modes) existed above this frequency. Based on expression (6), and with prior knowledge of the bottom loss vs. grazing angle function F, for this scenario the allowable range extent Δr becomes about 1100 m for 75 Hz and 420 m for 500 Hz, and so the 500 m range span was judged to be marginally adequate. This same scenario was used for the new demonstrations which are the subject of the present work.

4.1 Tonals Only

Tonal data was the subject of an inversion using the matched-slope technique. For convenience of the demonstration, the number and placement of tonals was selected so that the frequency span of values existing after matched-slope averaging, and available for further processing, would be continuously populated with data. In regard to the concepts of section 3.1, this requires a sufficiently dense spacing of tonals such that the frequency span Δf_t corresponding with the spread of the data from one tonal overlaps with data from one other tonal. The spacing between pairs of tonals to ensure a minimum degree of overlap is just $< \Delta f_t \approx f \, \Delta r / r$. For a range span Δr of 500 m, and nominal range r of 3750 m, the following tonals were sufficient to fill the band 75 to 500 Hz at the completion of matched-slope averaging at range 4000 m: 75 Hz, 84 Hz, 94 Hz, 105 Hz, 118 Hz, 132 Hz, 148 Hz, 166 Hz, 186 Hz, 209 Hz, 235 Hz, 264 Hz, 296 Hz, 332 Hz, 373 Hz, 419 Hz, 470 Hz and 527 Hz. Now, a mean-squared pressure T $(\text{Pa})^2$ of a tonal of at 1 m

range will be spread over a band of width $\Delta f_t \approx f\,\Delta r/r$ at range *r*. Taking into account both the *TL* to range *r*, and the width of the band Δf_t at range *r*, the mean-squared pressure spectral density at range *r* will be $T\,r/\left(f\,\Delta r\,10^{(TL/10)}\right)\ (\text{Pa})^2/\text{Hz}$. If this mean-squared pressure spectral density is to be the same as if the ocean was insonified by a broadband source radiating $B\ (\text{Pa})^2/\text{Hz}$ at 1 m, it follows that $T = f\,B\,\Delta r/r$. To achieve an equivalence to the received levels from a broadband source of *SL* 0.0 dB re $(1\,\mu\text{Pa})^2/\text{Hz}$, the *SL* values of the tonals were then set to $10\log_{10}(f\,\Delta r/r)$.

The resultant spectrum of received data, from matched-slope averaging of data received at the above tonals, is shown in Figure 3 (a). Here data from overlapping tonals is summed incoherently. This spectrum compares well with that in Figure 3 (b), which was obtained by the same process using the received coherent data of Figure 1 (a). Due to the choice of *SL* values of the tonals, the data in Figure 3 (a) are identical to values of *TL*. Figure 3 (b) also shows *TL* values as this was obtained from the *TL* data in Figure 1 (a). The value of Δf_h obtained by the autocorrelation of the amplitude data in Figure 3 (a) was 5.8 Hz and from Equation (4), the bottom loss vs. grazing angle slope *F* was determined as 8.4 dB/radian, which is close to the known value of 10 dB/radian. For data in Figure 3 (b), a value of 5.7 Hz was obtained for Δf_h, giving a value *F* of 8.3 dB/radian.

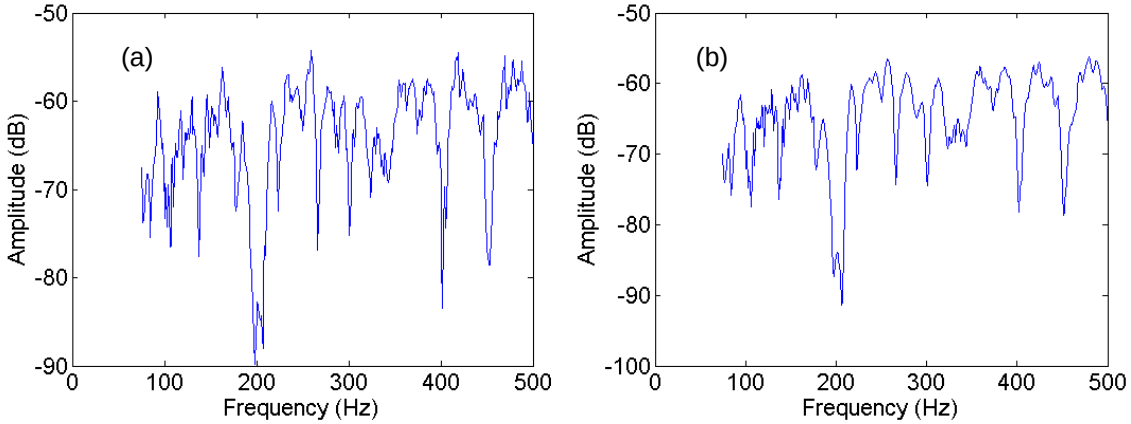

Figure 3 Received Level vs. frequency after matched-slope averaging over range 3.5 – 4 km, using (a) tonals (b) striations data in Figure 1 (a)

Whilst the spacings of the data in these sub-figures are very similar, the data obtained from the tonals has more fluctuations over small frequency scales. It is believed that this is due to the abrupt change in level (3 dB) as tonals overlap in short segments of the spectrum. Although not pursued here, it is obvious that data from just one tonal may be used for inversion if the frequency span Δf_t associated with the tonal after matched-slope averaging is >>Δf_h.

4.2 Random Broadband Signal in Ambient Noise

The receipt of random signals from the noise source is made against interference from ocean ambient noise. To demonstrate the effectiveness of the matched-slope processing of the data from a random source (ref. Figure 1 (b)) in a noisy environment, simulations were carried out for different levels of signal to noise ratio. This was defined as the ratio, expressed in dB, of the mean-squared pressure averaged over the spectrum of broadband signal received, and the mean-squared pressure of broadband noise. Each noise sample was obtained by generating an uncorrelated Gaussian value of sound pressure according to an appropriate value of mean-squared pressure, for each frequency and range bin. Each mean-squared noise value was then added to the respective mean-squared received signal value, for each range-frequency bin shown in Figure 1 (b). Matched-slope averaging was carried out on the resultant range-frequency data.

Figure 4 (a) shows the resultant spectrum of received data, after matched-slope averaging over 500 m centred at 3750 m range, for an SNR value of 5 dB. The spectrum (a) compares extremely

well with that in (b), which was obtained by the same process using the received data of Figure 1 (b) with zero noise. (The received signal values in (b) correspond with values of *TL*, as the data in Figure 1 (b) are *TL* values.) The value of Δf_h obtained from the amplitude data in Figure 4 (a) was 6.2 Hz giving a value *F* of 9.0 dB/radian, which is close to the known value of 10 dB/radian. For noiseless data in Figure 4 (b), the corresponding values were Δf_h = 5.9 Hz, *F* = 8.6 dB/radian. Clearly at SNR of 5 dB, the technique is not greatly impaired.

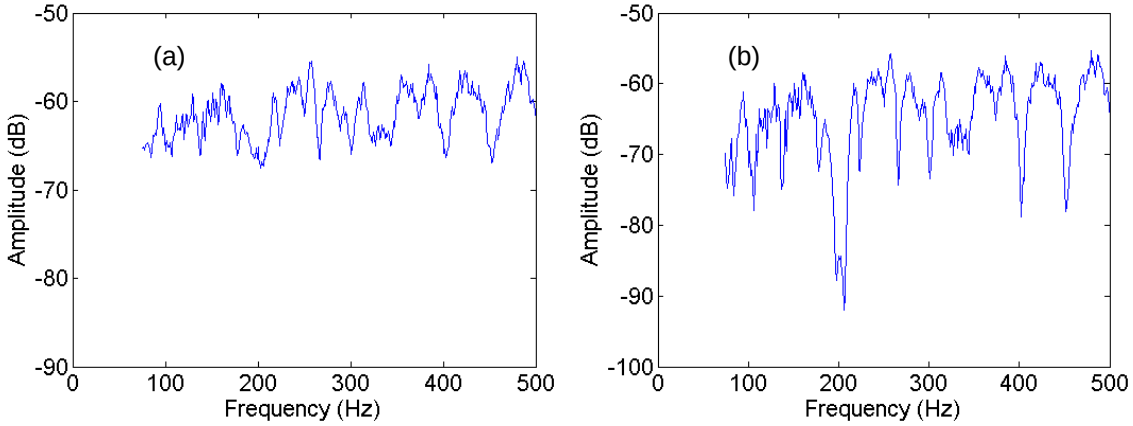

Figure 4 Received Level vs. frequency after matched-slope averaging over range 3.5 – 4 km, using (a) random signal data in noise for SNR 5 dB, (b) random signal data in Figure 1 (b)

4.3 Random Signal plus Tonals from Radially-Separated Source

As described in section 3.1, signals received from tonals and the random broadband signal received from a ship-of-opportunity may be assumed to undergo uncorrelated range fluctuations if the respective sources are separated in a radial direction by >> Δr_h. Signals received from tonals will then interfere with the received broadband signal in the conduct of the matched-slope averaging. There may be several source locations for the tonals, but only one source location was assumed here. From Equation (7), it follows that Δr_h = 90 m at the nominal range 3750 m for a frequency 300 Hz for the coarse sand seafloor of reflectivity *F* of 10 dB/radian. For the test scenario, such a separation will result in nearly correlated fluctuations at 75 Hz, but uncorrelated fluctuations at 500 Hz. The *SL* values chosen for the simulation were such that the received frequency data existing after matched-slope averaging was dominated by the data from the random source, to the extent of an average of 5 dB at all frequency values. This was achieved by using the same combination of tonals as used in section 4.1, but with a *SL* value for each respective tonal which was 5 dB less, while the *SL* values for the broadband random source were as used for Figure 1 (b). The effective SNR is then 5 dB at 500 Hz, diminishing to zero near 75 Hz.

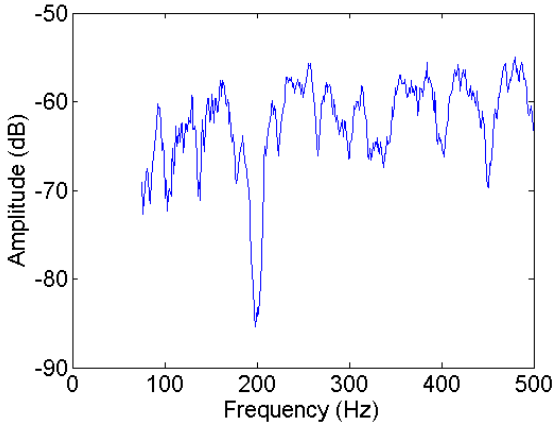

Figure 5 Received Level vs. frequency after matched-slope averaging over range 3.5 – 4 km, using random signal data in Figure 1 (b) plus tonals for SNR 5 dB, random signal dominating

Figure 5 shows the resultant spectrum of received data, after matched-slope averaging over 500 m centred at 3750 m range. At low frequencies, the spectrum compares well with that in Figure 4 (b), which was obtained using the received random data, only. However, at higher frequencies some spectrum features, particularly the nulls, are subject to interference from the tonals, as expected. This interference is similar to that provided by ambient noise, in Figure 4 (a), for which the SNR is also 5 dB. The value of Δf_h obtained from the amplitude data in Figure 5 was 6.35 Hz giving a value *F* of 9.2 dB/radian, which is close to the known value of 10 dB/radian. Again, the technique is not greatly impaired.

5 CONCLUSIONS

The impact of ambient noise, and of tonal data, on inverting the seafloor reflectivity parameter *F* dB/radian using range-frequency striation data from a random source in a shallow ocean has been studied briefly. The technique used for processing received data is the spectral variability method published previously by the authors. For practical measurement ranges and lower frequencies of interest, unless the seafloor is extremely reflective to sound, both broadband and tonal sound sources on a ship-of-opportunity may be assumed co-located, and the inversion will not be hindered by received tonals. If the received tonals have large amplitude, there is potential for inversion using the tonal data, only. At higher frequencies, the received tonals may interfere with an inversion based on received broadband signals. With sufficient averaging over range, each of ambient noise and interfering tonals have been shown to have a limited impact on inversion for SNR of 5 dB.

6 REFERENCES

1. A. D. Jones and P. A. Clarke, “Rapid seafloor inversion in shallow oceans using broadband acoustic data”, Proceedings of 20th ICA, Sydney, Australia, 23-27 August 2010
2. A.D. Jones, P.A. Clarke and D.W. Bartel, *Rapid Determination of Seafloor Acoustic Reflectivity by Exploiting Frequency Variability within Striations Data*, Proceedings of OCEANS’13 San Diego, 23-26 September 2013, San Diego, USA
3. D. W. Bartel, “HANKEL: A Tool for Exploring the Complex Pressure Field in Range-Independent Underwater Acoustic Environments”, Proceedings of 20th ICA, Sydney, Australia, 23-27 August 2010.
4. F. B. Jensen and W. A. Kuperman, “Optimum frequency of propagation in shallow water environments”, J. Acoust. Soc. Am., vol. 73, March, pp. 813-819, 1983.
5. L. M. Brekhovskikh and Yu. P. Lysanov, Fundamentals of Acoustics, 3rd edition, Springer-Verlag, New York, 2003.
6. P. J. Smith, Jr., “The Averaged Impulse Response of a Shallow-Water Channel”, J. Acoust. Soc. Am., vol. 50, no. 1, pp. 332-336, 1971.
7. M. K. Prior and C. H. Harrison, “Estimation of seabed reflection loss properties from direct blast pulse shape (L)”, J. Acoust. Soc. Am. vol. 116 no. 3, pp. 1341-1344, 2004.
8. R.J. Urick, “Intensity Summation of Modes and Images in Shallow-Water Sound Transmission” *J. Acoust. Soc. Am.* 46, No. 3 (Part 2), 780-788 (1969)
9. M. R. Schroeder, “Frequency-Correlation Functions of Frequency Responses in Rooms”, J. Acoust. Soc. Am., vol. 34, no. 12, pp 1819-1823, 1962
10. A. D. Jones, G. J. Day and P. A. Clarke, “Single parameter description of seafloors for shallow oceans”, Proceedings of Acoustics’08 Paris, Paris, France, 29 June – 4 July, pp 1725 – 1730, also published in Proceedings of the 9th European Conference on Underwater Acoustics, *ECUA 2008*, volume 1, pp 161 – 166, 2008.
11. Urick, R. J. *Intensity Summation of Modes and Images in Shallow-Water Sound Transmission*, J. Acoust. Soc. Am., Vol. 46, No. 3 (Part 2), 1969, pp 780-788